https://doi.org/10.5194/egusphere-2026-5131
Preprint. Discussion started: 3 September 2026

Seasonal stratification controls on vertical nutrient exchange in a High Arctic fjord (Inglefield Bredning, NW Greenland)

Anna Pedersen[1,2*], Steffen M. Olsen[1], Carolin R. Löscher[2]

[1] Danish Meteorological Institute, Copenhagen, Denmark

[2]Nordcee, University of Southern Denmark, Odense, Denmark

Correspondence to: Anna Pedersen (aped@dmi.dk)

Abstract. High Arctic fjords are changing rapidly under ongoing global warming yet remain comparatively understudied despite their sensitivity to shifts in sea ice, ocean temperature, and glacier dynamics. In northwest Greenland, Inglefield Bredning is influenced by marine-terminating glaciers and exchange with Baffin Bay and the North Water polynya, making it a representative system for assessing how physical changes in the Arctic propagate into fjord biogeochemistry. Here, we investigate how seasonal stratification develops across winter, spring, and early summer, and how it regulates vertical nutrient exchange and biological activity. A persistent Atlantic Water layer below ~220 m occupies the fjord year-round, forming a stable reservoir of heat and nutrients that defines the background hydrographic structure. However, strong vertical stratification limits exchange between this deep nutrient reservoir and the euphotic zone, where nutrient concentrations remain low throughout the year. Upper-water-column nutrient concentrations are higher in winter than in early summer, but do not indicate complete winter homogenization with deeper waters. Pronounced spatial variability along the fjord further reflects the influence of marine-terminating glaciers, with localized hydrographic modification suggesting that glacier-driven processes may intermittently enhance vertical nutrient supply. Chlorophyll concentration peak in summer, consistent with strong biological uptake under increasingly stratified conditions. Together, these results indicate that productivity in Inglefield Bredning is governed not by the magnitude of the deep nutrient reservoir itself, but by the availability if macronutrients and the physical processes controlling their transfer to the euphotic zone. As Arctic warming strengthens stratification while altering glacier dynamics and sea ice cover, future productivity in high Arctic fjords will depend critically on the evolving balance between mechanisms that restrict and promote vertical nutrient supply.

1 Introduction

Climate change is transforming the Arctic at a rate unmatched by any other region of the world, with profound consequences for ocean circulation, sea-ice cover, glacier mass loss, and marine biogeochemical cycling. Increasing atmosphere and ocean temperatures have accelerated the retreat of the Greenland Ice Sheet and Arctic glaciers, reduced seasonal sea-ice extent, and

https://doi.org/10.5194/egusphere-2026-5131
Preprint. Discussion started: 3 September 2026

altered the exchange of heat, freshwater, nutrients, and carbon between the atmosphere and the ocean (Arrigo et al., 2008; Straneo and Heimbach, 2013; Ardyna and Arrigo, 2020). These changes are reshaping marine ecosystems across the Arctic through their influence on water column stratification, vertical mixing, nutrient supply, and primary production. While Arctic Ocean primary production has generally increased in recent decades, largely owing to longer open water seasons and reduces sea ice cover (Arrigo and van Dijken, 2015; Lewis et al., 2020; Ardyna and Arrigo, 2020), enhanced freshwater input from sea ice melt and glacial discharge also strengthens upper ocean stratification, potentially limiting nutrient replenishment to surface waters and creating considerable regional variability in ecosystem responses (Li et al., 2009; Coupel et al., 2015; Mills et al., 2018; Zhu et al., 2019).

Arctic fjords are among the environments where these climate driven changes are expressed most directly. Although they occupy only a small fraction of the global ocean, fjords form highly dynamic interfaces between the open ocean, the cryosphere, and the atmosphere, where relatively small changes in water mass properties or vertical micing can rapidly alter physical and biogeochemical conditions (Iriarte et al., 2014; Straneo and Cenedese, 2015; Kanna et al., 2018; Hopwood et al., 2020; Meire et al., 2023). In Greenland, fjords serve as the primary conduits through which freshwater, sediment, and ice discharged from the Greenland Ice Sheet reach the coastal ocean, making them key locations for glacier–ocean interactions and important regulators of regional carbon and nutrient cycling (Iriarte et al., 2014; Straneo and Cenedese, 2015; Hopwood et al., 2020; Meire et al., 2023). Their hydrography is governed by the interaction of Atlantic and Arctic-derived water masses, seasonal sea ice, freshwater runoff, and glacial discharged creating strong spatial and seasonal gradients in stratification, circulation and ecosystem productivity.

Many Greenlandic fjords, particularly along the southeast and northwest coasts, are influenced by marine-terminating glaciers that have undergone rapid retreat in recent decades in response to ocean warming (Gardner et al, 2013; Khan et al., 2010; Rignot et al., 2012; Straneo and Heimbach, 2013). Where bathymetry allows, warm Atlantic Water penetrates fjords at depth and reaches glacier termini enhancing submarine melting while strongly influencing fjord circulation and nutrient transport (Straneo et al., 2012). The type and magnitude of glacial influence fundamentally shape ecosystems. Fjords fed by marine-terminating glaciers generally support higher biological productivity than those influenced by land-terminating glaciers because buoyant subglacial discharge entrains nutrient- and iron-rich deep waters into the euphotic zone, sustaining phytoplankton growth throughout summer despite strong stratification (Hopwood et al., 2016; Meire et al., 2017; Kanna et al., 2018; Meire et al., 2023). At the same time, glacial discharge can increase turbidity, reduce light availability, dilute surface nutrient concentrations, and modify the marine carbonate system by lowering total alkalinity and carbonate ion concentrations, thereby influencing carbon cycling within fjords and adjacent coastal waters (Howe et al., 2010; Doney et al., 2009; Fransson et al., 2015, 2023; Stedmon et al., 2023; Henson et al., 2024). Consequently, the balance between enhanced nutrient supply and increased stratification, light limitation and carbonate chemistry changes determine the biogeochemical response of individual fjord systems.

Despite their recognized importance, observations that resolve the seasonal evolution of hydrography, stratification, nutrient availability, and biological productivity in Greenlandic fjords remain limited, particularly during winter and early

https://doi.org/10.5194/egusphere-2026-5131
Preprint. Discussion started: 3 September 2026

spring when pre-bloom conditions are established (Wassmann et al., 2011; Wassmann, 2015; Schuback et al., 2017). This lack of year-round observations limits our understanding of how ongoing climate change will alter the coupled physical and biogeochemical dynamics of fjord systems and their role within the wider Arctic marine environment. We investigate the seasonal variability in stratification and nutrient availability in a high Arctic fjord in northwest Greenland. Using four field campaigns spanning winter, spring and early summer, we examine hydrographic structure, water mass properties, and circulation in Inglefield Bredning (Fig. 1), with a particular focus on the development and strengthening of stratification under the combined influence of seasonal landfast sea ice cover, the warm Atlantic Water penetrating the fjord at depth and marine-terminating glaciers. Hydrographic observations include temperature, salinity, oxygen concentration, and fluorescence, complemented by analyses of macronutrients and trace metals (dissolved iron).

1.1 Study region and background

Fieldwork was conducted in Inglefield Bredning, a fjord in northwestern Greenland that stretches approximately 100 km in length and 15-20 km in width, reaching depths exceeding 900 m (Willis et al., 2018; Podolskiy and Sugiyama, 2020, Fig. 1). The fjord is influenced by multiple marine-terminating glaciers, and its hydrography is shaped by the presence of both local and Atlantic water masses, a seasonal land-fast ice cover, and the absence of shallow sills, which allows for deep exchanges with Baffin Bay.

The fjord is classically covered by landfast sea ice from early November through to July, but recent years this season has shortened, and land-fast sea ice only forms late December and break up in June, in line with observation from the Arctic also showing shorter seasons of sea ice cover (Meier and Stroeve, 2022). Ice thickness typically reaches 100-120 cm at the end of the winter season. In the dry Arctic tundra climate, snow cover on the ice exceeds 10-15 cm only in late spring. The air temperature during the field campaigns varies from -34°C during winter (December and January) and spring (March) to 0°C in early summer (June).

https://doi.org/10.5194/egusphere-2026-5131
Preprint. Discussion started: 3 September 2026

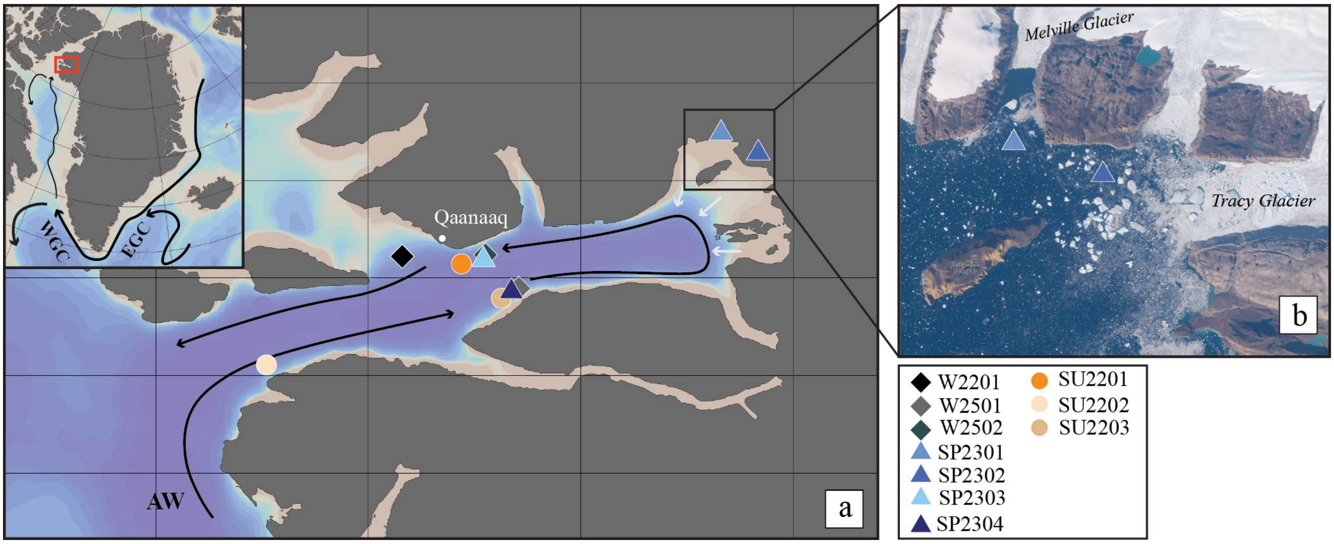

Figure 1: a) map of the study region (Inglefjeld Bredning) identifying the sample stations, b) showing the location of the sample stations in relation to the Melville and Tracy Glacier. Satellite photo (Sentinel II L1C, True Colour) from the ice-free season in 2023 (2nd of September) from the Copernicus Sentinel web browser (https://browser.dataspace.copernicus.eu/). Black arrows indicating ocean currents, light grey arrows indicate glacial meltwater flow direction (based on Willis et al., 2018). WGC: West Greenland Current, EGC: East Greenland Current, AW: Atlantic Water.

This study is based on hydrographic observations and biogeochemical samples made during four field campaigns in June 2022, December 2022, March 2023 and January 2025 (Fig. 1). Sample locations can be seen on Figure 1, where the winter (W) samples are annotated WXXYY (XX: sample year, YY: sample no; black and grey diamonds), spring (SP) samples are annotated SPXXYY (blue triangles), and summer (SU) samples are annotated SUXXYY (orange circles).

Though spanning three seasons, these observations are all from the ice-covered period, with new land fast sea ice formed in January and isothermal, 'rotten' ice still acting as a thermostat on surface layer temperatures in June. The field work is organized from the DMI Geofysisk Observatorium in Qaanaaq, managed by the Danish Meteorological Institute (DMI), and the sample locations are reached by dog sleds across the sea ice with the support of local hunters in all seasons, where the June 2022 campaign took place only a week before the breakup of the land fast sea ice.

The width of Inglefield Bredning exceeds the local Rossby radius of deformation by a factor of 2-4, allowing for three-dimensional circulation, with predominantly counterclockwise surface flow (Willis et al., 2018). Atlantic Water (AW) enters the fjord at depth, originating from the West Greenland Current, a warm extension of the Irminger Current that moves poleward along the western Greenlandic shelf guided by topography and at the latitude of Davis Strait, subducted below polar waters. By the time it reaches Inglefield Bredning, this water mass has cooled to temperatures of 0.5°to 1.5°C and forms a temperature core at 300-350 m depth in the fjord (Willis et al., 2018; Table 1; Fig. 2). Above the AW a modified Atlantic water mass is usually present (mAW), which is formed by mixing and dilution of the AW from below. The surface layer in the extended ice-covered period studied here exhibits strong seasonal variability, either with properties of the Winter Layer (WL)

https://doi.org/10.5194/egusphere-2026-5131
Preprint. Discussion started: 3 September 2026

or a local Winter Layer (lWL) with much lighter and fresher properties (Table 1; Fig. 2). The AW and to some extent the WL water masses flow into the fjord along its southern boundary, progress toward the fjord head where they interact with glaciers and topography (forming the mAW), and exit along the northern boundary (Willis et al., 2018; black arrows in Fig. 1). The WL is formed by dynamic sea ice processes in the north water polynya. Two sampling sites (SP2301 and SP2302) are located downstream of the Melville and Tracy glaciers, within surface waters influenced by glacial meltwater (Fig. 1b; Fig. 4).

Table 1: Water masses in Inglefjeld Bredning

Water mass	Temperature	Salinity
Atlantic Water (AW)[a]	>0.5°C	33.8–34.2
Modified AW (mAW)	-0.75–0.5°C	33.4–33.8
Winter Layer (WL)	<0°C	32.0–33.4
Local Winter Layer (lWL)	<-1.5°C	<33.8

a: Willis et al., 2018

2 Methods

2.1 CTD profiles and nutrient samples

Water mass profiles were obtained using a winch-driven pumped CTD (Seabird SBE19plusV) equipped with auxiliary sensors including oxygen (SBE43 sensor, USA), fluorescence (Seapoint) and turbidity (Seapoint) at all sampling stations and seasons (Fig. 1). All sensors are recently factory calibrated, within a year, but no other in-situ calibration has been performed on the sensor data including fluorescence, turbidity and oxygen. In the following fluorescence is used as a representative for phytoplankton biomass in the upper water column. Sensor accuracy is 0.001°C for temperature and 0.01 for salinity. The oxygen is calibrated to an accuracy of 2% (saturation) but only used here as an indicator for recently ventilated waters. It should be noted that the SBE43 oxygen sensor does not tolerate the temperatures encountered during the field campaign and has been kept warm in between deployments. Turbidity and fluorescence (biomass) accuracy is not estimated.

Water samples for nutrients and dissolved iron were collected at each sampling station using a 2.7 L Niskin bottle attached to a line and closed by a drop-messenger at pre-selected depths. The samples were collected from 1, 12 and 50 m depth. Due to extreme cold and varying weather conditions subsampling of collected water samples for individual parameters was done partly in the field and partly at the field station.

In March 2023, part of the sampling was done during a six-day expedition, where a transportable lab was used to enable sampling and processing in the field despite the low temperatures. Samples from station SP2301 were sampled into blue-cap bottles at the sampling station, and subsequently they were transported to the Camp lab located at station SP2302 and processed. The transportable Camp lab was heated to about 10°C to prevent the samples from freezing for filtrations. Samples from sampling station SP2302 were sampled into blue-cap bottles and then further sampled and processed within one hour in the Camp lab (a tent heated to about 10°C). At sampling stations SP2303 and SP2304, samples were filled into blue cap bottles and transported back to the field station for further sampling and processing.

https://doi.org/10.5194/egusphere-2026-5131
Preprint. Discussion started: 3 September 2026

In January 2025 all samples were sampled into 2L and 1L blue cap bottles and further processed at the field station.

2.2 Sample analysis

2.2.1 Nutrient concentrations

Samples for nutrient analysis, nitrate (NO_3^-), nitrite (NO_2^-) and phosphate (PO_4^{3-}) were taken in 2ml triplicates and stored at -18°C until further analysis in Denmark (Nordcee, University of Southern Denmark). Concentrations were determined spectrophotometrically (Thermo Scientific, Genesys 1OS UV-VIS spectrophotometer) following established protocols Murphy and Riley (1962) for $PO_4^{3-}$and García-Robledo et al. (2014) for nitrate and nitrite.

2.2.2 Trace metal concentrations

Samples were analysed for concentrations of dissolved trace metals, here focusing on dissolved iron using an Agilent 7900 Quadrupole Inductively Coupled Plasma (ICP) Mass Spectrometers instrument (Agilent Technologies). Calibration standards (20, 40, 60 80, and 100 mg L^{-1}) were prepared in 2% nitric acid from 1000 mg L^{-1} ICP standards. Samples were prepared in 2% nitric acid and stored at room temperature until further analysis (Olesik, 2013). Trace metal samples only are only available from the March 2023 campaign.

https://doi.org/10.5194/egusphere-2026-5131
Preprint. Discussion started: 3 September 2026

3 Results

3.1 Variability in ocean circulation, hydrography and water masses

3.1.1 Circulation and water masses of the fjord

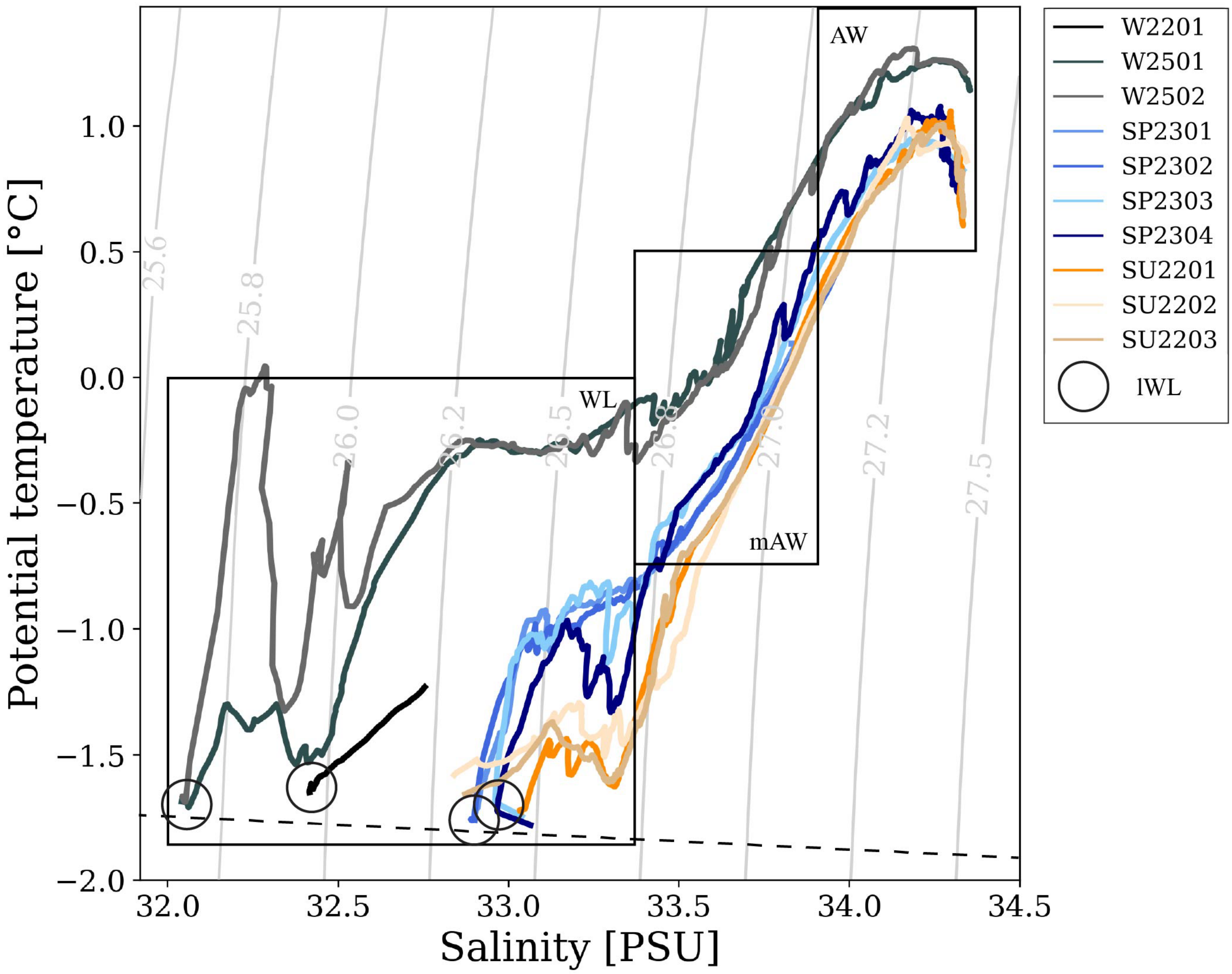

Figure 2: T/S plot showing the different water masses and the seasonal distribution of the sample stations through winter 2022 (black line) and 2025 (grey lines), spring 2023 (blue lines) and summer 2022 (orange lines). AW: Atlantic Water, mAW: modified Atlantic Water, WL: winter layer, lWL: local winter layer. AW is defined based on Willis et al., 2018. Black dashed line shows the freezing point curve.

Four water masses are typically present in the Inglefield Bredning: a cold and fresh local winter layer (lWL), a saltier winter layer (WL), the warm and salty Atlantic Water layer (AW), and the modified Atlantic Water (mAW; Fig. 2, Table 1). The N-S transect of the mid-fjord stations illustrates that the AW is present at depth (below 220 m) through-out the year (Fig. 3). The transect shows that the winter water column is occupied by lWL in the top 50 m, followed by WL until 130 m, whereafter the

https://doi.org/10.5194/egusphere-2026-5131
Preprint. Discussion started: 3 September 2026

modified water mass mAW is present until 220 m depth, as AW occupies the depth of the water column. In winter, the water mass distribution is horizontally uniform distributed across the fjord. The spring transect differs from the winter transect as the depth of the water masses are shallower on the southern side of the fjord compared to the northern side (Fig. 3b). During spring, the WL forms a lens in the surface layer on the northern side of the fjord, reflecting the cold and relatively salty surface water runoff from the glaciers in the head of the fjord. Below the WL, mAW is present until 210 m depth along the northern margin and 180 m depth along the southern margin, whereafter AW occupies the depth of the fjord. During summer, the water mass depth distribution across the fjord is smoothened out, yet the WL lens is still evident in the section plot (Fig. 3c). The WL occupies the top 90-100 m (southern and northern margin respectively), while the mAW layer thickens and occupies the water column until 220 m, where AW is present.

https://doi.org/10.5194/egusphere-2026-5131
Preprint. Discussion started: 3 September 2026

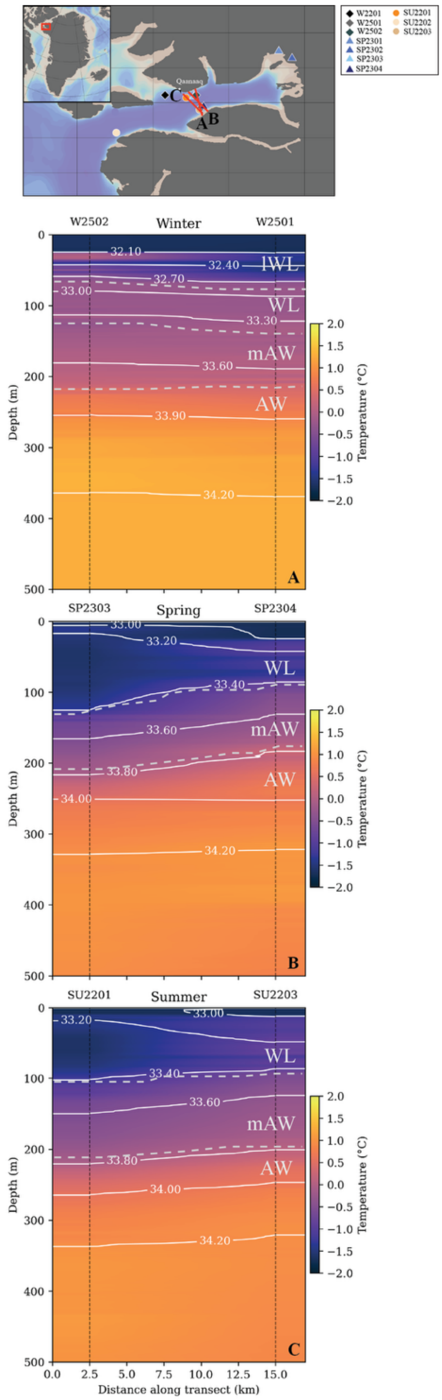

Figure 3: North–South transects (red lines on map) of the mid fjord from winter (A; January 2025), spring (B; March 2023) and summer (C; June 2022) showing the temperature distribution of the water column. Salinity contours are added (white contours). Light grey dashed lines indicate water mass boundaries as highlighted by labels, WL: winter layer, lWL: local winter layer, mAW: modified Atlantic water, AW: Atlantic Water (see Table 1 for specific water mass properties). N and S indicate north and south in the transect.

https://doi.org/10.5194/egusphere-2026-5131
Preprint. Discussion started: 3 September 2026

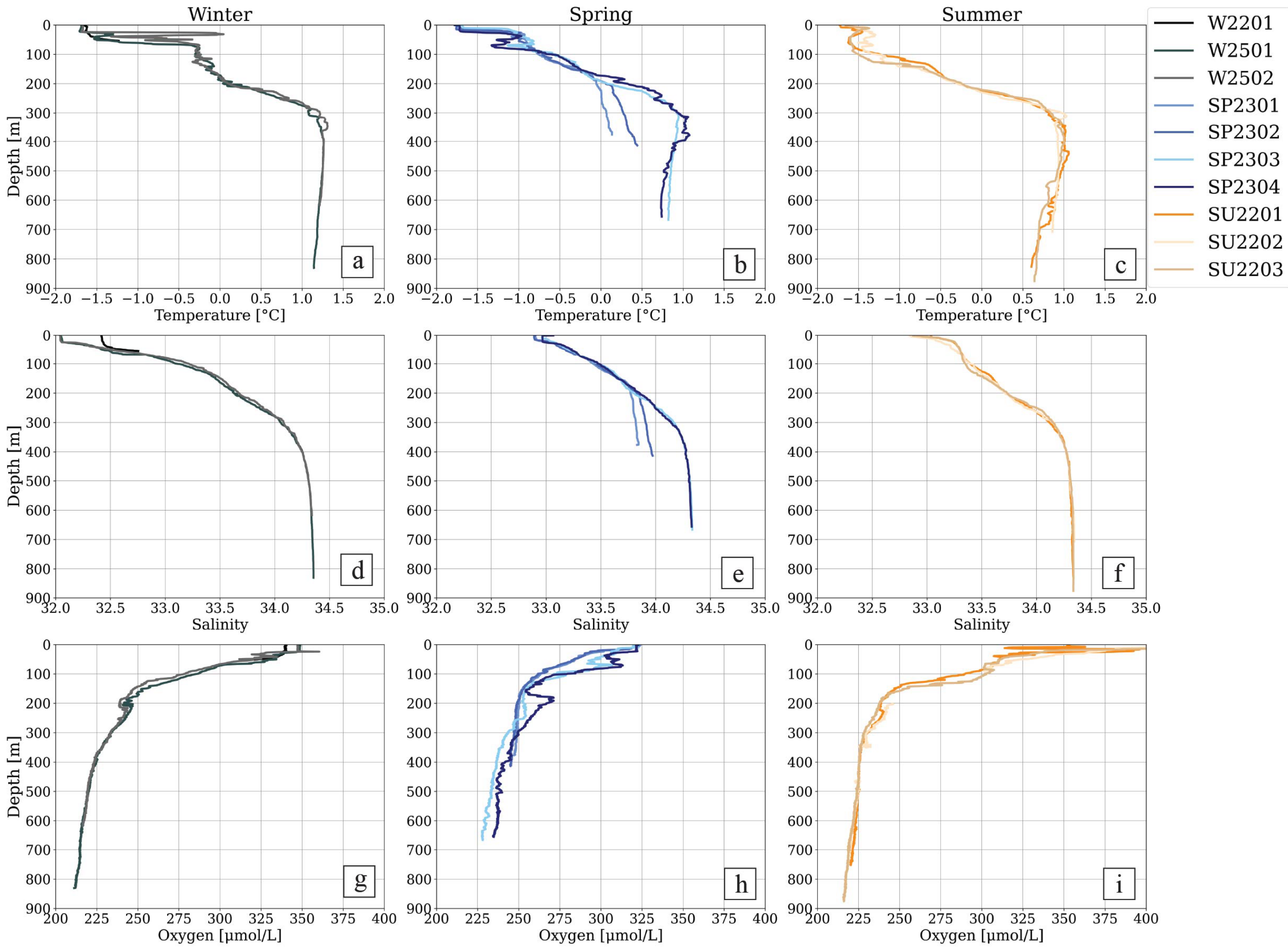

Figure 4: Full depth profiles of temperature (a-c), salinity (d-f) and oxygen (g-i) for winter (a,d,g), spring (b,e,h) and summer (c,f,i) from CTD casts.

The full CTD profiles further corroborates the interpretations from the fjord transect and water mass analysis (Fig. 4d-f). The December 2022 (W2201) winter sample location is located in a shallow region of the main fjord, due to sea-ice break up in the main fjord the days before the field campaign. These profiles therefore do not extend to the depth of the AW. Here, we only see the local cold and fresh winter layer (lWL, Fig. 4a,d, black line).

At the stations near the marine-terminating glaciers (SP2301, SP2302) the core of the AW cannot be identified (Fig. 4b,e), instead, at these depths, a modified Atlantic derived water mass (mAW) is found, colder and fresher, in part explained by interactions with the marine-terminating glaciers and extensive mélange area in front of the most prominent glaciers. On top of the AW, the mAW is generally present at all locations sampled from 80-220 m in winter (Fig. 4a,d) and 100-220 metres in spring (Fig. 4b,e) and 110-250 metres in summer (Fig. 4c,f). Lastly, we see the WL present in the surface 100-110 metres in winter, spring and summer (Fig. 4a,d). During winter, the top ~50 m is occupied by the cold and fresh lWL, which is formed

https://doi.org/10.5194/egusphere-2026-5131
Preprint. Discussion started: 3 September 2026

by local processes related to sea ice forming within the fjord. It differs from the WL by being more fresh and cold, where the WL is formed by processes in the polynya-region outside of Inglefield Bredning.

3.1.2 Stratification in the surface layer

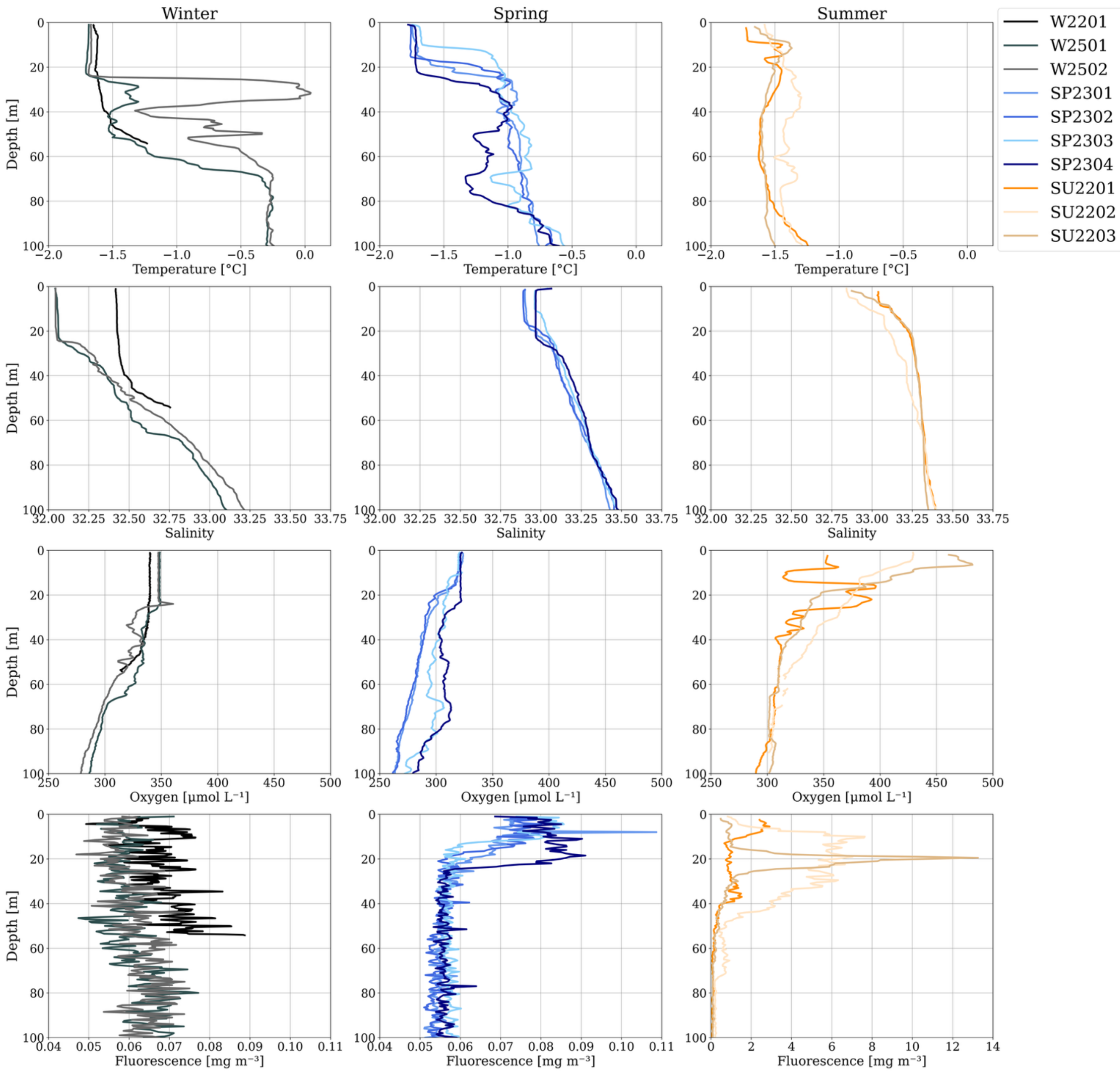

195 **Figure 5:** Seasonal profiles of temperature (a-c), salinity (d-f), oxygen (g-i), and fluorescence (j-l) showing the quantitative variability of the size of chl max along the varying stratification of the top 100 metres of the water column.

https://doi.org/10.5194/egusphere-2026-5131
Preprint. Discussion started: 3 September 2026

Focusing on the details of the upper stratification in the winter layers of the fjord, including the size and position of distinct water layers and the chlorophyll maximum (hereafter chl max), reveals seasonal variability (Fig. 5). During winter (both December 2022 and January 2025), the water column exhibited a well-mixed surface layer extending to approximately 25 m depth, within the definition of the winter layers and with temperatures close to the freezing point of sea water (Fig. 5a,d). Within this layer, temperatures remained below -1.6°C. Surface salinity was lower in January 2025 (~32.10) compared to December 2022 (~32.40), and oxygen concentrations were correspondingly higher (~348 µmol (92% saturation) L^{-1} versus ~340 µmol L^{-1} (88% saturation); Fig. 5g). Below the under-ice mixed layer, a pronounced halocline and thermocline were present. At the coastal and shallow December 2022 station (55 m water depth), temperature increased to -1.22°C, salinity reached 32.75 and oxygen declined to 317 µmol L^{-1}. In January 2025, the thermocline extended from ~22 to 80 m depth, with spatial variability between the southern (W2502) and northern (W2501) stations (Fig. 5d). In winter we see low phytoplankton biomass (fluorescence 0.05 to 0.09 mg/m^3) evenly distributed in the surface layer revealing no chl max (Fig. 5j).

During spring the well-mixed surface layer extends to varying depths across stations, the deepest being at SP2304 on the southern inflow branch of the fjord, where it reaches 25 m, and the shallowest being 10 m at SP2303 (Fig. 5b,e,h), at the northern outflow side of the fjord. The layer is occupied by WL, which is expected to be formed by cooling, ice formation and associated brine rejection within the fjord on the northern flank and reflecting more the open water conditions outside the fjord on the southern flank of the fjord. Within the well-mixed surface layer in spring, the temperature was close to freezing point at -1.7 to -1.78°C (Fig. 5 b). Surface salinity was lower closer to the glacier (stations SP2301 and SP2302) where the salinity was ~32.90 compared to the mid-fjord stations (SP2303 and SP2304) where salinity was ~32.97 (Fig. 5e), corroborating the view that the layer is gradually modulated by brine in time and space. Additionally, the oxygen profile shows a well-oxygenated surface layer of ~320 µmol L^{-1} (~82% saturation), where after the oxygen profiles diverge with depth: the near-glacier stations (SP2301 and SP2302) being less oxygenated than the mid-fjord stations (SP2303 and SP2304; Fig. 5k). In spring we also see a distinct halocline and thermocline present below the cold mixed winter layer. The thermocline and halocline extend to 30 m, temperatures increasing to -1.0°C and salinity to 33.1. During spring we observe the highest concentration of phytoplankton biomass at the near-glacier station SP2301 reaching 0.11 mg/m^3 at 9 m depth. The mid-fjord station SP2304 show a deeper and wider chl max reaching 0.091 between 15-25 m (Fig. 5k).

In summer, the surface mixed layer becomes markedly shallower, yet the surface is still occupied by WL (Fig. 5c,f,i), while the top of the water column is more strongly stratified than in winter and spring. A well-mixed surface layer is limited to the upper 5–8 m at the northern mid-fjord station (SU2201) and the mouth-fjord station (SU2202) likely representing a new layer decoupling from the winter mixed layer by the input at surface of freshwater from the melting sea ice. This layer is not clearly evident at the southern mid-fjord station (SU2203). Below this thin surface layer, a sharp halocline and thermocline develop within the upper 10–12 m, accompanied by strong vertical gradients in temperature, salinity, and oxygen. Surface waters remain near the freezing point (−1.7 to −1.6°C), while temperatures increase to −1.4 to −1.3°C immediately below the halocline. Oxygen concentrations are highest in the surface layer, particularly at SU2202 and SU2203 (supersaturated, <100% saturation), and decrease rapidly with depth (Fig. 5i).

https://doi.org/10.5194/egusphere-2026-5131
Preprint. Discussion started: 3 September 2026

Summer profiles show pronounced and spatially variable chl maxima (Fig. 5l). At SU2201, the chl max is shallow and confined to the upper 10 m, with a modest peak in fluorescence concentration of ~2.8 mg m^{-3}. In contrast, SU2202 exhibits a deeper and broader chl max extending from ~7 to 48 m, reaching a maximum of 7.8 mg m^{-3}. The highest phytoplankton biomass is observed at SU2203, where the chl max is concentrated between 18 and 28 m depth and peaks at 13.2 mg m^{-3}. These differences indicate strong spatial heterogeneity in summer phytoplankton biomass distribution, associated with enhanced stratification and reduced vertical mixing.

Figure 6 illustrates how the thermal stratification of the water column develops from winter to early summer in 2023. In this region water column density stratification primarily derives from differences in salinity of the water masses, due to the relative small vertical difference in temperature. However, the data used for figure 6 is obtained from ice-tethered moored instruments (MicroCAT C-T sensors (SBE-37-SI) and RBRsolo[4] temperature loggers), deployed at fixed depths (3, 10, 20, 30, 40, 60, 90, 120, 150, 200, 250, 300m), where the majority of the instruments measures temperature and only a few measures salinity, therefore in this case the thermal stratification of the water column will provide a more detailed view of the stratification in the fjord. During winter, the water column was characterized by relatively homogenous temperatures in the upper water column, suggesting weak thermal stratification and potential enhanced vertical mixing. Thermal stratification strengthens from spring and onwards as the cold surface layer become increasingly separated from warmer subsurface waters.

https://doi.org/10.5194/egusphere-2026-5131
Preprint. Discussion started: 3 September 2026

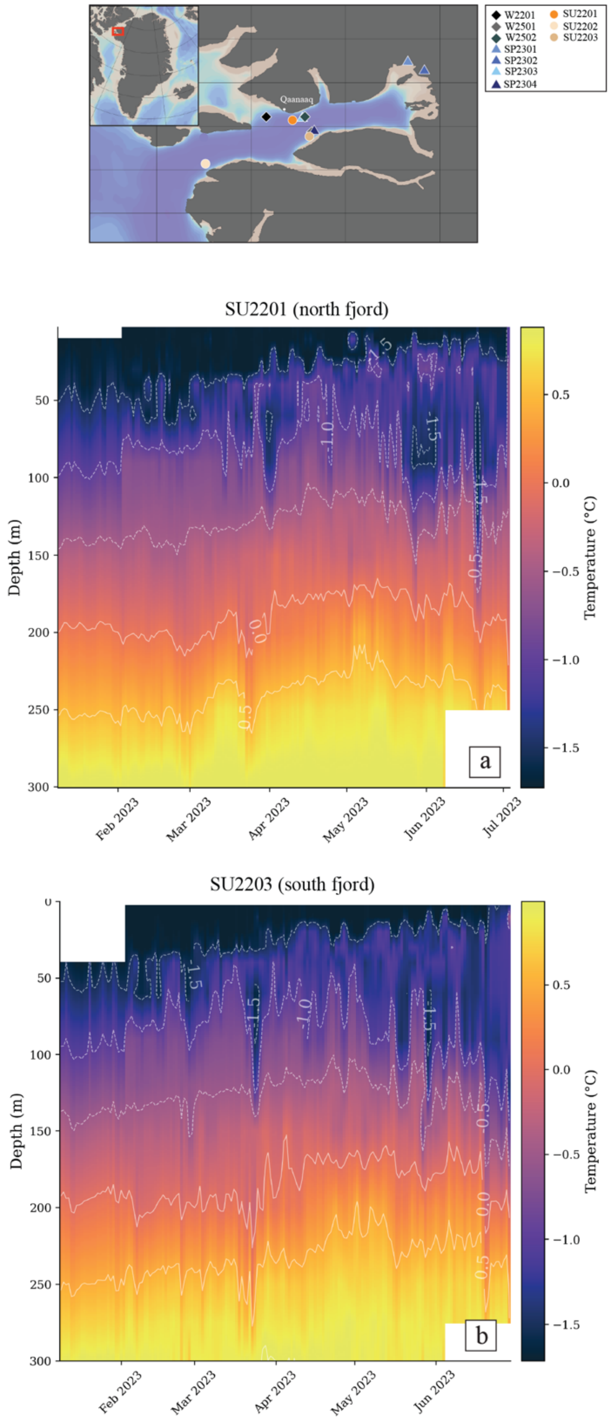

Figure 6: Hovmøller plot of the temperature through the water column illustrating the development of the stratification from January 2023 to July 2023. A) showing the north side of the fjord, and b) showing the southern side of the fjord. White full contours show positive °C while dashed contours show negative °C.

https://doi.org/10.5194/egusphere-2026-5131
Preprint. Discussion started: 3 September 2026

3.2 Variability in nutrient availability

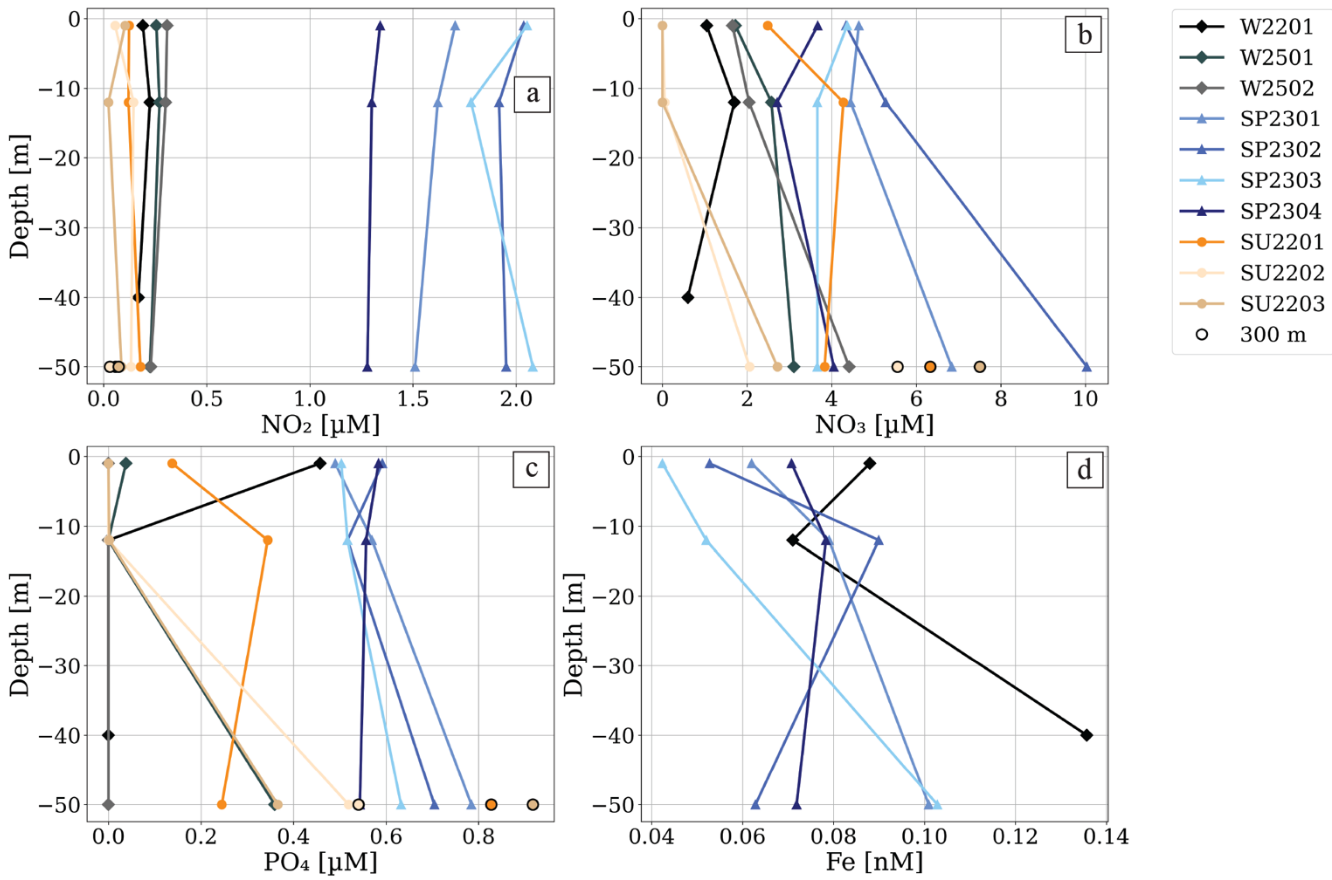

Figure 7: Spatial and temporal variability in a) nitrite (µM), b) nitrate (µM) and c) phosphorus (µM) availability, d) dissolved iron concentrations for winter and spring samples. Early summer samples marked by a black circle are samples taken from 300 m depth (AW core), plotted at the 50 m depth to enhance comparison with the surface layers.

In general, nutrient concentrations exhibited pronounced seasonal variability, with higher availability in winter and spring and reduced concentrations in summer, alongside spatial variability within the fjord (Fig. 7).

During winter, nutrient concentrations remained moderate and show limited vertical variability, indicating incomplete replenishment following drawdown during both summer and into fall (Fig. 7a-c). Surface nitrite concentrations range from 0.19 to 0.30 µM and were similar to values at 12 m (0.23-0.30 µM) and 40-50 m depth (0.17-0.23 µM; Fig. 7a). Nitrate concentrations were slightly higher, ranging from 1.05 to 1.72 µM at the surface and increasing to 0.6-4.4 µM at depth (Fig. 7b). Phosphorus concentrations were comparatively low in winter, with surface values between 0.04 and 0.46 µM and similarly low concentrations at depth (Fig. 7c). Surface dissolved iron concentration during winter 2023 was 1.58 nM (1 m), increasing to 2.43 nM at depth (40 m).

https://doi.org/10.5194/egusphere-2026-5131
Preprint. Discussion started: 3 September 2026

In spring, concentrations of all measured nutrients were highest across depths, indicating that the spring bloom has not yet substantially depleted nutrient availability (Fig. 7a-c). Oxygen levels in the surface waters also do not reach super saturation values (%saturation values!), which will be expected later in the season along with nutrient depletion. The weakening stratification following spring allows for increased vertical nutrient exchange, where the locations close to the glaciers (SP2301 and SP2302) indicate increased nutrient influx from the AW water mass (Fig. 7 and 8). Nitrite concentrations ranged from 1.3 to 2.1 µM throughout the upper 50 m (Fig. 7a), while nitrate concentrations increased to 3.7–4.6 µM at the surface and reached up to 10.0 µM at 50 m depth (Fig. 7b). Phosphorus concentrations were also elevated in spring, with values of 0.49-0.59 µM at the surface and up to 0.78 µM at depth (Fig. 7c). Spring sampling was conducted closer to the glacier front, where meltwater input may have influenced nutrient distributions within the fjord. Near the glaciers the primary nutrients show a stronger increase with depth possibly indicating buoyancy driven upwelling. Surface concentration of dissolved iron ranges from 0.76–1.27 nM (1 m), and increases to 1.13–1.84 nM at depth (50 m).

During summer, nutrient concentrations within the local mixed layer were reduced relative to spring, while concentrations below the halocline within the winter layers (Fig. 5d,e,f) remained higher, consistent with biological uptake and strong stratification limiting vertical nutrient resupply (Fig. 5c,f,i; Fig. 7d). However, none of the measured nutrients were fully depleted. Nitrite concentrations decreased to 0.05-0.12 µM at the surface and remained low throughout the upper 50 m. At depth (300 m, AW core), the early summer samples show a low concentration in nitrite (0.06 µM; Fig. 7a), while both nitrate and phosphorous show high concentrations compared to the surface layer (6.33 and 0.83 µM respectively; Fig 7b+c), illustrating that the AW works as a reservoir for nutrients at depth in the fjord. We have no data for dissolved iron from early summer.

Comparing the NO_x (nitrite + nitrate pool) to the phosphorus inventory illustrates another temporal variability in the nutrient availability (Fig. 8). Winter samples (black and grey diamonds) show generally lower phosphorus concentrations compared to NO_x. Spring samples (blue triangles) show slightly lower NO_x compared to phosphorus. Summer samples (orange circles) show greater variability, the surface samples centred around the Redfield ratio or slightly lower Nox compared to phosphorus. The deep summer samples (black outlined circles) reflect the higher nutrient concentrations at depth. The spring samples located near the glaciers (outlined by red circles) show similar NO_x to phosphorus ratio as the deep summer samples, which illustrates that the AW is mixed into the surface layer near the glaciers during early summer. Figure 8 also illustrates how the samples follow a linear depletion from summer to winter and spring, yet we do not see any nutrient limitation in this fjord system.

https://doi.org/10.5194/egusphere-2026-5131
Preprint. Discussion started: 3 September 2026

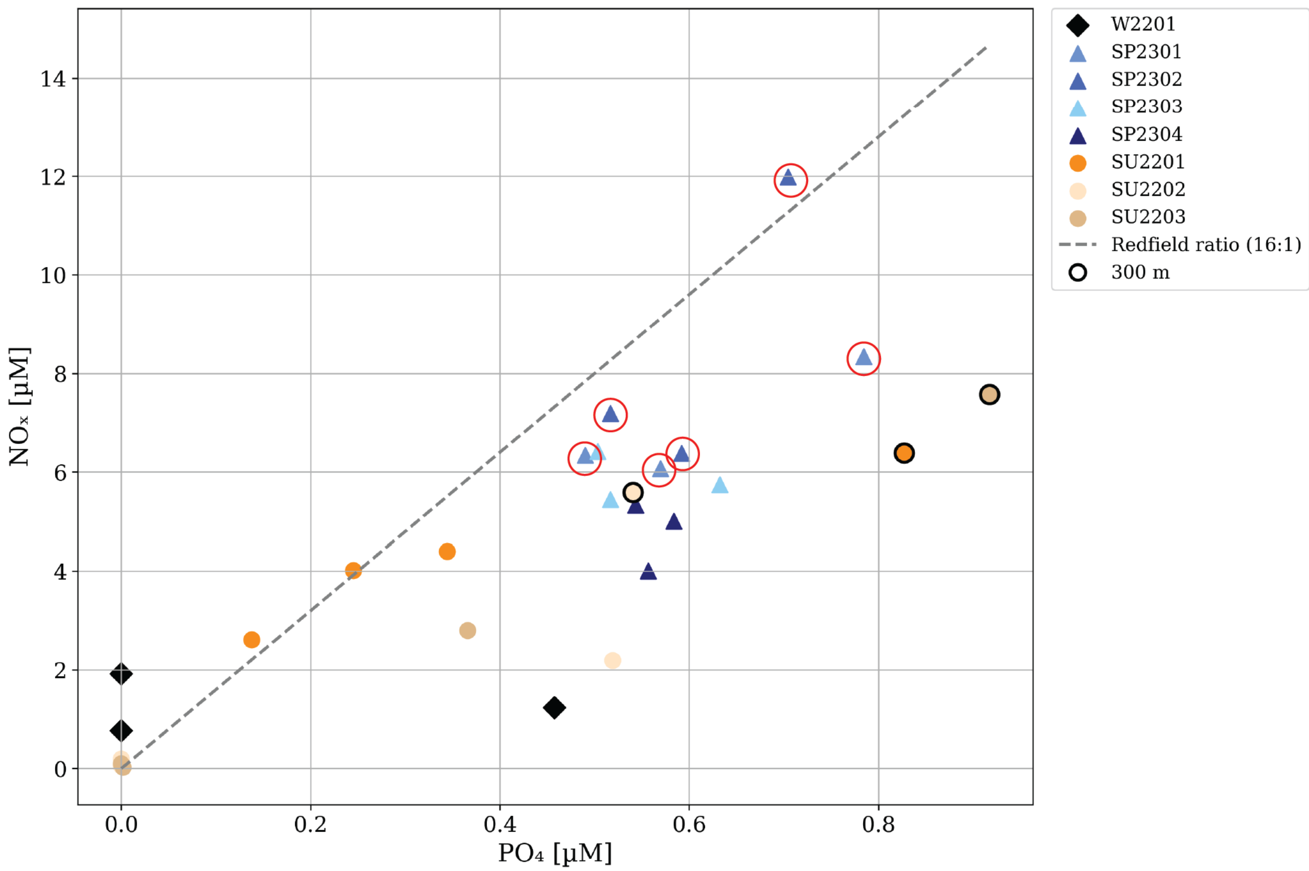

295 **Figure 8:** NOx/PO4 ratio plot demonstrating the ratio between NOx and PO4 in all the sample stations. Full grey line shows the trend line of the ratio between all the samples, where the dashed grey line shows the ideal Redfield Ratio (16:1). Red circles indicate samples close to the glaciers, while black circles indicate the deep 300 m samples.

4 Discussion

4.1 Fjord-scale circulations, water mass structure and vertical exchange

300 Our observations reveal a persistent presence of Atlantic Water (AW) below approximately 220 m throughout all three seasons (Figs. 3 and 4), indicating sustained deep-water renewal and connectivity between Inglefield Bredning and Baffin Bay. The fjord sill depth allows AW to occupy the deepest layers, where it remains thermally distinct and forms a stable deep reservoir of heat and nutrients. Beneath the seasonal surface layer, this persistent AW maintain a year-round vertical density gradient relative to the overlying waters.

305 In contrast, the upper water column exhibits pronounced seasonal variability that strongly regulates vertical exchange processes. During winter, the surface layer is characterized by cold and relatively fresh Winter Layers (WL and lWL; Figs. 3 and 4). Despite surface cooling, stratification persists due to the halocline structure, while ice cover surpasses wind driven

https://doi.org/10.5194/egusphere-2026-5131
Preprint. Discussion started: 3 September 2026

mixing. Although brine rejection during sea ice formation weakens stratification relative to summer, vertical mixing remains limited to a shallow mixed layer of approximately 20 m, preventing deep ventilation and maintaining separation between the surface layer and the underlying AW.

With the transition to spring, increasing solar radiation initiates biological activity while the upper water column becomes more stratified in both temperature and salinity (and density). Mixed layer depth shows spatial variability (Fig. 5), reflecting local ventilation processes and circulation. The onset of a phytoplankton bloom is evident from increasing chlorophyll maxima, particularly at the mid-fjord station SP2304 and the near-glacier station SP2301 (Fig. 5 k). However, nutrient concentrations indicate that surface waters are not yet deleted, suggesting that recent or intermittent mixing has supplied nutrient to the euphotic zone prior to the establishment of stronger stratification.

By early summer, the mixed layer shoals substantially and stratification intensifies (Fig. 5). Sharp vertical salinity gradients develop, strongly suppressing vertical exchange and isolating the surface layer from deeper nutrient reservoirs. As a result, the influence of AW in surface biogeochemistry remains largely indirect and depends on episodic or seasonally enhanced mixing events capable of bridging the persistent density structure.

In addition to seasonal variability, stratification and vertical exchange also vary spatially in response to fjord scale circulation. AW enters at depth along the southern margin, while interactions with marine-terminating glaciers at the fjord head introduce buoyancy at depth, driving upwelling and export of modified Atlantic waters (mAW) along the northern margin. Stations near the glaciers (SP2301 and SP2302, Fig. 5) exhibit enhanced upper ocean stratification and shallower mixed layers compared to mid-fjord stations (SP2303 and SP2304, Fig. 5), indicating that freshwater input and glacier-driven processes modulate mixing at sub-fjord scales. Although there is no clear evidence of buoyant plumes reaching the surface in our dataset, the observed hydrographic heterogeneity suggests a localized influence of glacier driven circulation non the vertical exchange.

Overall, the fjord is characterized by distinct and persistent stratification that decouples the nutrient rich AW from the euphotic zone. While AW provides a substantial reservoir of heat and nutrients, its contribution to surface productivity is constrained by limited vertical exchange. This decoupling is consistent with observations from other High Arctic fjords and the broader Arctic Ocean, where freshwater inputs from sea ice and glacial processes enhance stratification and restrict mixing (e.g. Kim et al., 2025; Juranek, 2022; Hopwood et al., 2020). Similarly, studies from fjords such as Godthåbsfjord (SW Greenland) and Kongsfjorden (Svalbard) demonstrate that freshwater input can both strengthen stratification and locally enhance vertical exchange through buoyant plume dynamics (Cottier et al., 2005; Meire et al., 2017), highlighting the complex and spatially variable controls on mixing in Arctic fjord systems.

4.2 Seasonal nutrient dynamics

The observed seasonal variability in nutrient concentrations reflects the combined influence of stratification and biological uptake. Vertical exchange sets the initial nutrient inventory of the surface layer, while biological processes progressively modify it throughout the growth season.

https://doi.org/10.5194/egusphere-2026-5131
Preprint. Discussion started: 3 September 2026

In winter, nutrient concentration in the upper water column are high relative to early summer, but do not indicate complete homogenization with deeper waters (Fig. 7). This incomplete replenishment supports the interpretation of limited winter overturning, likely limited by persistent haline stratification and reduced wind-driven mixing under sea ice. Although surface cooling slightly weakens thermal stratification, the freshwater-controlled density structure maintains partial decoupling from the nutrient-rich AW at depth. Consequently, the winter nutrient inventory represents only partial renewal of surface concentrations.

During spring, in particular the mixed layer nutrient concentrations reach seasonal maxima (Fig. 7a-c), consistent with recent vertical replenishment and the early phase of the bloom prior to peak drawdown. Increasing light availability initiates rapid biological uptake, and nutrient concentrations begin to decline in tandem with increasing chlorophyll. Stations near the glaciers (SP2301 and SP2302) exhibit elevated nitrate concentrations both at the surface and at depth compared to mid-fjord stations (SP2303 and SP2304; Fig. 7a-c), indicating enhanced exchange with the deeper reservoirs by upwelling and possibly by enhanced mixing due to complex local topographic features. In the season's studies, only the early summer nutrient concentrations may reflect input from surface runoff.

By summer, strong stratification and a shallow mixed layer restrict vertical nutrient supply, and biological uptake dominates surface nutrient dynamics. Surface nitrate concentrations decline to low levels (Fig. 7a-c), while high nitrate persists in the underlying Atlantic layers (Fig. 7a-c black outlined circles), highlighting the persistent vertical separation between nutrient demand in the euphotic zone and supply at depth. This seasonal decoupling of the surface layer underscores the central role of mixing efficiency in sustaining productivity beyond the spring bloom.

Surface nitrate conditions in Inglefield Bredning during summer (0-5 µM in the upper ~12 m) are comparable to those reported from Godthåbsfjord in August 2013 (Meire et al., 2017). There are major dynamical differences between Inglefield and Godthåbsfjord, where tidal mixing of water masses is a key feature of the latter. Still, observations in both fjords show surface nitrate depletion concurrent with elevated concentrations at depth, consistent with strong biological uptake and limited or insufficient vertical resupply. Meire et al. (2017) propose that subglacial discharge acts as an important mechanism for nutrient resupply in Godthåbsfjord. Buoyant meltwater plumes entrain large volumes of nutrient-rich saline fjord water during their ascent (Bendtsen et al., 2015; Mortensen et al., 2011; Sciascia et al., 2013), subsequently settling beneath the low-salinity surface layer and generating subsurface cold-water anomalies. Such plume-driven nutrient uplift is not clearly resolved in the sparse CTD profiles available from Inglefield Bredning, suggesting either temporal variability in plume activity or a more localized influence than captured by our sampling. Nevertheless, the spatial patterns observed in spring support the interpretation that glacier-driven processes can modulate stratification and vertical exchange, even if their biogeochemical imprint varies across the fjord. Furthermore, Cottier et al. (2005) describes how Arctic fjords (e.g. Kongsfjorden in Svalbard) have strong seasonal stratification driven by freshwater input and sea ice processes, similar to our observations in Inglefield Bredning. Both these studies show how seasonal ice cover suppresses wind mixing and vertical nutrient resupply, causing incomplete replenishment of the surface layer in winter.

https://doi.org/10.5194/egusphere-2026-5131
Preprint. Discussion started: 3 September 2026

A notable feature of the seasonal cycle is the shift in relative nutrient limitation. Winter conditions appear relatively phosphorous-poor, whereas summer conditions shift toward comparatively NO_x-poor surface waters (Fig. 8). Low temperatures reduce the rate at which organic phosphorous is remineralised to inorganic phosphate, while the winter supply of fresh organic matter and external phosphate if also low. Consequently, the regeneration of phosphate may not compensate for its previous biological consumption (Glud, 2008; Chandler and Mackie 2020). Such seasonal changes in nutrient stoichiometry may influence phytoplankton community compositions, competitive dynamics, and recycling efficiency, with potential implications for carbon export and ecosystem structure. The early summer deep-water samples (300m depth) show high concentrations of nutrients compared to the surface water samples (Fig. 7 and 8). Furthermore, we see how the spring samples close to the marine-terminating glaciers are closer to the deep-water sample stoichiometry, indicating that the surface layer near the glaciers is supplied with nutrients from the deep reservoir in the AW layer. The summer samples show lower NOx than spring, consistent with post-bloom nutrient depletion.

Trace metal concentration represented by dissolved iron concentrations fall within the range reported for other high-arctic fjord systems, including the 79°N Glacier fjord in northeast Greenland (1.07 – 1.79 nM; Krause et al., 2021), and remain above depletion levels in the available samples (Fig. 7d). Although summer dissolved iron measurements are not available, the observed high summer biomass and sustained macronutrient drawdown argue against strong iron limitation during the productive season. Instead, the data suggest that macronutrients availability and physical stratification exert primary control over productivity in this system. Notably, dissolved iron concentration reported for Inglefield Bredning in August 2017 (~4 nM; Kanna et al., 2020) exceed our spring values by more than a factor of two, indicating potential interannual variability but further supporting the view that trace metal scarcity is unlikely to be the dominant constraint on primary production.

4.3 Implications for seasonal productivity and future changes in High Arctic fjords

Rapid Arctic climate change is reshaping the physical structure and biological functioning of high-arctic fjord systems. Inglefield Bredning is likely to experience continued sea ice loss, rising seawater temperatures, and altered freshwater input driven by glacial retreat and enhanced meltwater discharge. These changes may promote earlier seasonal stratification and longer open-water periods, potentially extending the phototrophic growing season. However, stronger and more persistent stratifications may simultaneously reduce vertical nutrient resupply, limiting the availability of nitrate in surface waters and constraining sustained productivity (Tremblay et al., 2015; Zhu et al., 2019; Li et al., 2009; Coupel et al., 2015; Mills et al., 2018).

The net effect of sea ice decline on primary production remains uncertain. Some studies report enhanced productivity associated with a retreating sea ice edge and increased light availability (Frey et al., 2021; Møller et al., 2023; Ardyna and Arrigo, 2020), whereas others suggest that reduced nutrient supply under stronger stratification may ultimately suppress production (Hayward et al., 2025). Despite these contrasting projections, there is broad agreement that continued sea ice loss, shorter ice-covered seasons, and thinning ice will fundamentally alter the seasonal productions regime of Arctic fjords. Our

https://doi.org/10.5194/egusphere-2026-5131
Preprint. Discussion started: 3 September 2026

results underscore that the outcome will depend not only on light availability, but critically on the balance between stratifications and vertical exchange.

Glacier dynamics add a further layer of complexity. As demonstrated by Meire et al. (2017), marine-terminating glaciers can strongly influence fjord biogeochemistry, not through direct nitrate input from meltwater, but by modifying hydrography. Buoyant subglacial discharge plumes entrain nutrient-rich deep water as they rise, enhancing vertical exchange and sustaining summer productivity. In systems where such plume-driven upwelling is active, marine-terminating glaciers may therefore act as indirect regulators of nutrient supply during periods of strong stratification.

Widespread thinning and retreat if marine-terminating glaciers have been documented along the Greenland ice sheet as a consequence of submarine and atmospheric melt (Carr et al., 2013; Howat and Eddy, 2011; Meire et al., 2017). While many glaciers in northern and northeastern Greenland currently terminate in deep, submarine basins, retreat above sea level remains a plausible future scenario in other regions. A transition from marine-terminating to land-terminating systems would likely reduce plume-driven upwelling and weaken this localized nutrient resupply mechanism, potentially leading to reduces summer productivity. Conversely, as long as glaciers remain marine-terminating, their influence on fjord hydrography and nutrient exchange may partially counteract the stratifications-driven isolation of surface waters.

Taken together, our observations form a present-day baseline for understanding future productivity of Inglefield Bredning and similar High Arctic fjords will be governed by evolving balance between increasing stratification and mechanisms that enhance vertical exchange. Whether climate change ultimately amplifies or suppresses biological production will depend on how these competing processes interact.

5 Conclusions

Together, our observations demonstrate that Inglefield Bredning functions as a stratified High Arctic fjord in which Atlantic Water forms a persistent, nutrient-rich deep reservoir that remains largely decoupled from the euphotic zone. Seasonal variations in mixed-layer depth and stratification regulate the efficiency of vertical exchange, allowing partial nutrient replenishment in winter and early spring but leading to pronounced surface isolation during summer. As a result, nutrient dynamics reflect a tight coupling between physical structure and biological uptake: incomplete winter renewal, spring maxima associated with recent mixing, and strong summer depletion under shallow stratification. Spatial heterogeneity near marine-terminating glaciers further indicates that glacier-driven processes may locally modulate mixing and nutrient availability, even when plume signals are not directly resolved in the dataset. Overall, productivity in the fjord is governed less by the absolute size of the deep nutrient reservoir than by the episodic and seasonal processes capable of bridging the persistent density structure that separates supply at depth from demand at the surface.

Code and data availability

CTD profile data and mooring data is available upon request. Nutrient and trace metal data will be available at Pangaea.

Author contributions

AP, CRL and SMO designed and organised the field work. AP and SMO carried out the field work. AP performed most of the data analysis, with supervision from SMO and CRL. AP wrote the manuscript, while CRL and SMO contributed to the revision of the manuscript.

Competing interests

The authors declare that the research was conducted in the absence of any commercial or financial relationships that could be construed as a potential conflict of interest.

Acknowledgements

The field work was executed with the invaluable help from local hunters in all four field campaigns. They provided dog sleds, safety, logistics and contributed to the data collection. The local hunters include Qillaq Danielsen, Gustav Simigaq, Gedion Kristiansen, Peter Avike, Quma Kvist and Mikile Kristiansen. Furthermore, the authors would like to acknowledge Aksel Ascanius for helping with logistics in Qaanaaq. Lastly, we would like to acknowledge Zarah Koefod and Erik Laursen and Isabell Schlangen for analysing samples and assisting in the lab.

Financial support

AP was supported by SDU's climate cluster and the Villum Foundation (grant no. 29411) and by Danmarks Fri Forskningsfond (DFF, Carolin R. Löscher, grant no. 4283-00265B). SMO has received funding from the European Union's Horizon 2020 research and innovation programme under grant agreement No. 101003472 (Arctic Passion).

References

Ardyna, M. and Arrigo, K.R.: Phytoplankton dynamics in a changing Arctic Ocean. Nature Climate Change, 10(10), pp.892-903, https://doi.org/10.1038/s41558-020-0905-y, 2020.

Arrigo, K.R. and Van Dijken, G.L.: Continued increases in Arctic Ocean primary production. *Progress in oceanography*, *136*, pp.60-70, 2015.

Arrigo, K.R., van Dijken, G.L. and Bushinsky, S.: Primary production in the Southern Ocean, 1997–2006. Journal of Geophysical Research: Oceans, 113(C8), https://doi.org/10.1029/2007JC004578, 2008.

Bendtsen, J., Mortensen, J. and Rysgaard, S.: Modelling subglacial discharge and its influence on ocean heat transport in Arctic fjords. Ocean Dynamics, 65(11), pp.1535-1546, 2015.

Carr, J.R., Stokes, C.R. and Vieli, A.: Recent progress in understanding marine-terminating Arctic outlet glacier response to climatic and oceanic forcing: Twenty years of rapid change. Progress in Physical Geography, 37(4), pp.436-467, 2013.

Chandler, D. and Mackie, S.: Observations of late-winter marine microbial activity in an ice-covered fjord, west Greenland. *Earth System Science Data*, *12*(2), pp.897-906, 2020.

Cottier, F., Tverberg, V., Inall, M., Svendsen, H., Nilsen, F. and Griffiths, C.: Water mass modification in an Arctic fjord through cross-shelf exchange: The seasonal hydrography of Kongsfjorden, Svalbard. Journal of Geophysical Research: Oceans, 110(C12), 2005.

Coupel, P., Ruiz-Pino, D., Sicre, M.A., Chen, J.F., Lee, S.H., Schiffrine, N., Li, H.L. and Gascard, J.C.: The impact of freshening on phytoplankton production in the Pacific Arctic Ocean. Progress in Oceanography, 131, pp.113-125, https://doi.org/10.1016/j.pocean.2014.12.003, 2015.

Doney, S.C., Fabry, V.J., Feely, R.A. and Kleypas, J.A.: Ocean acidification: the other CO2 problem. Annual review of marine science, 1(1), pp.169-192, https://doi.org/10.1146/annurev.marine.010908.163834, 2009.

Fransson, A., Chierici, M., Nomura, D., Granskog, M.A., Kristiansen, S., Martma, T. and Nehrke, G.: Effect of glacial drainage water on the CO_2 system and ocean acidification state in an Arctic tidewater-glacier fjord during two contrasting years. Journal of Geophysical Research: Oceans, 120(4), pp.2413-2429, https://doi.org/10.1002/2014JC010320, 2015.

Fransson, A., Chierici, M., Granskog, M.A., Dodd, P.A. and Stedmon, C.A.: Impacts of glacial and sea-ice meltwater, primary production, and ocean CO2 uptake on ocean acidification state of waters by the 79 North Glacier and northeast Greenland shelf. Frontiers in Marine Science, 10, p.1155126, https://doi.org/10.3389/fmars.2023.1155126, 2023.

Frey, K.E., Comiso, J.C., Cooper, L.W., Grebmeier, J.M. and Stock, L.V., 2021. Arctic ocean primary productivity: The response of marine algae to climate warming and sea ice decline. Arctic Report Card, DOI: 10.25923/kxhb-dw16, 2021.

Gardner, A.S., Moholdt, G., Cogley, J.G., Wouters, B., Arendt, A.A., Wahr, J., Berthier, E., Hock, R., Pfeffer, W.T., Kaser, G. and Ligtenberg, S.R.: A reconciled estimate of glacier contributions to sea level rise: 2003 to 2009. science, 340(6134), pp.852-857, https://doi.org/10.1126/science.1234532, 2013.

Kim, H., Han, D., Park, S.R. and Kim, T.H.: Seasonal interplay of water mass mixing and nutrient dynamics in an Arctic fjord: a case study of Kongsfjorden, Svalbard. Ocean Science, 21(6), pp.3089-3103, 2025.

García-Robledo, E., Corzo, A. and Papaspyrou, S.: A fast and direct spectrophotometric method for the sequential determination of nitrate and nitrite at low concentrations in small volumes. Marine Chemistry, 162, pp.30-36, https://doi.org/10.1016/j.marchem.2014.03.002, 2014.

Glud, R.N.: Oxygen dynamics of marine sediments. *Marine Biology Research*, *4*(4), pp.243-289, 2008.

Hayward, A., Wright, S.W., Carroll, D., Law, C.S., Wongpan, P., Gutiérrez-Rodriguez, A. and Pinkerton, M.H.: Antarctic phytoplankton communities restructure under shifting sea-ice regimes. Nature Climate Change, pp.1-8, https://doi.org/10.1038/s41558-025-02379-x, 2025.

Henson, H.C., Sejr, M., Meire, L., Sørensen, L.L., Winding, M.H. and Holding, J.M.: Resolving heterogeneity in CO_2 uptake potential in the Greenland coastal ocean. Journal of Geophysical Research: Biogeosciences, 129(12), https://doi.org/10.1029/2024JG008246, 2024.

Hopwood, M.J., Connelly, D.P., Arendt, K.E., Juul-Pedersen, T., Stinchcombe, M.C., Meire, L., Esposito, M. and Krishna, R.: Seasonal changes in Fe along a glaciated Greenlandic fjord. Frontiers in Earth Science, 4, p.15, https://doi.org/10.3389/feart.2016.00015, 2016.

Hopwood, M.J., Carroll, D., Dunse, T., Hodson, A., Holding, J.M., Iriarte, J.L., Ribeiro, S., Achterberg, E.P., Cantoni, C., Carlson, D.F. and Chierici, M.: How does glacier discharge affect marine biogeochemistry and primary production in the Arctic?. The Cryosphere, 14(4), pp.1347-1383, https://doi.org/10.5194/tc-14-1347-2020, 2020.

Howat, I.M. and Eddy, A.: Multi-decadal retreat of Greenland's marine-terminating glaciers. Journal of Glaciology, 57(203), pp.389-396, 2011.

Howe, J.A., Austin, W.E., Forwick, M., Paetzel, M., Harland, R.E.X. and Cage, A.G.: Fjord systems and archives: a review, https://doi.org/10.1144/SP344.2, 2010.

Iriarte, J.L., Pantoja, S. and Daneri, G.: Oceanographic processes in Chilean fjords of Patagonia: from small to large-scale studies. Progress in Oceanography, 129, pp.1-7, https://doi.org/10.1016/j.pocean.2014.10.004, 2014.

Juranek, L.W.: Changing biogeochemistry of the Arctic Ocean. Oceanography, 35(3/4), pp.144-155, 2022.

Kanna, N., Sugiyama, S., Ohashi, Y., Sakakibara, D., Fukamachi, Y. and Nomura, D.: Upwelling of macronutrients and dissolved inorganic carbon by a subglacial freshwater driven plume in Bowdoin Fjord, northwestern Greenland. Journal of Geophysical Research: Biogeosciences, 123(5), pp.1666-1682, https://doi.org/10.1029/2017JG004248, 2018.

Kanna, N., Sugiyama, S., Fukamachi, Y., Nomura, D. and Nishioka, J.: Iron supply by subglacial discharge into a fjord near the front of a marine-terminating glacier in northwestern Greenland. Global Biogeochemical Cycles, 34(10), p.e2020GB006567, 2020.

Khan, S.A., Wahr, J., Bevis, M., Velicogna, I. and Kendrick, E.: Spread of ice mass loss into northwest Greenland observed by GRACE and GPS. Geophysical Research Letters, 37(6), 2010.

Krause, J., Hopwood, M.J., Höfer, J., Krisch, S., Achterberg, E.P., Alarcón, E., Carroll, D., González, H.E., Juul-Pedersen, T., Liu, T. and Lodeiro, P.: Trace element (Fe, Co, Ni and Cu) dynamics across the salinity gradient in Arctic and Antarctic glacier fjords. Frontiers in Earth Science, 9, p.725279, https://doi.org/10.3389/feart.2021.725279, 2021.

Lewis, K.M., Van Dijken, G.L. and Arrigo, K.R.: Changes in phytoplankton concentration now drive increased Arctic Ocean primary production. *Science*, *369*(6500), pp.198-202, 2020.

Li, W.K., McLaughlin, F.A., Lovejoy, C. and Carmack, E.C.: Smallest algae thrive as the Arctic Ocean freshens. Science, 326(5952), pp.539-539, https://doi.org/10.1126/science.1179798, 2009.

Meier, W.N. and Stroeve, J.: An updated assessment of the changing Arctic sea ice cover. Oceanography, 35(3/4), pp.10-19, 2022.

Meire, L., Mortensen, J., Meire, P., Juul-Pedersen, T., Sejr, M.K., Rysgaard, S., Nygaard, R., Huybrechts, P. and Meysman, F.J.: Marine-terminating glaciers sustain high productivity in Greenland fjords. Global Change Biology, 23(12), pp.5344-5357, https://doi.org/10.1111/gcb.13801, 2017.

Meire, L., Paulsen, M.L., Meire, P., Rysgaard, S., Hopwood, M.J., Sejr, M.K., Stuart-Lee, A., Sabbe, K., Stock, W. and Mortensen, J.: Glacier retreat alters downstream fjord ecosystem structure and function in Greenland. Nature Geoscience, 16(8), pp.671-674, https://doi.org/10.1038/s41561-023-01218-y, 2023.

Mills, M.M., Brown, Z.W., Laney, S.R., Ortega-Retuerta, E., Lowry, K.E., van Dijken, G.L. and Arrigo, K.R.: Nitrogen limitation of the summer phytoplankton and heterotrophic prokaryote communities in the Chukchi Sea. Frontiers in Marine Science, 5, p.362, https://doi.org/10.3389/fmars.2018.00362, 2018.

Mortensen, J., Lennert, K., Bendtsen, J. and Rysgaard, S.: Heat sources for glacial melt in a sub-Arctic fjord (Godthåbsfjord) in contact with the Greenland Ice Sheet. Journal of Geophysical Research: Oceans, 116(C1), 2011.

Murphy, J.A.M.E.S. and Riley, J.P.: A modified single solution method for the determination of phosphate in natural waters. Analytica chimica acta, 27, pp.31-36, https://doi.org/10.1016/S0003-2670(00)88444-5, 1962.

Møller, E.F., Christensen, A., Larsen, J., Mankoff, K.D., Ribergaard, M.H., Sejr, M., Wallhead, P. and Maar, M.: The sensitivity of primary productivity in Disko Bay, a coastal Arctic ecosystem, to changes in freshwater discharge and sea ice cover. Ocean Science, 19(2), pp.403-420, https://doi.org/10.5194/os-19-403-2023, 2023.

Olesik, J. W.: Inductively Coupled Plasma Mass Spectrometers, Treatise on Geochemistry: Second Edition, 15, 309-336, 10.1016/B978-0-08-095975-7.01426-1, 2013.

Podolskiy, E.A. and Sugiyama, S.: Soundscape of a narwhal summering ground in a glacier fjord (Inglefield Bredning, Greenland). Journal of Geophysical Research: Oceans, 125(5), https://doi.org/10.1029/2020JC016116, 2020.

Rignot, E. and Mouginot, J.: Ice flow in Greenland for the international polar year 2008–2009. Geophysical Research Letters, 39(11), 2012.

Sciascia, R., Straneo, F., Cenedese, C. and Heimbach, P.: Seasonal variability of submarine melt rate and circulation in an East Greenland fjord. Journal of Geophysical Research: Oceans, 118(5), pp.2492-2506, 2013.

Schuback, N., Hoppe, C.J., Tremblay, J.É., Maldonado, M.T. and Tortell, P.D.: Primary productivity and the coupling of photosynthetic electron transport and carbon fixation in the Arctic Ocean. Limnology and Oceanography, 62(3), pp.898-921, https://doi.org/10.1002/lno.10475, 2017.

Stedmon, C., Henson, H., Henson, H.C., Holding, J.M., Meire, L., Rysgaard, S., Stedmon, C.A., Stuart-Lee, A., Bendtsen, J. and Sejr, M.: Coastal freshening drives acidification state in Greenland fjords, https://doi.org/10.1016/j.scitotenv.2022.158962, 2023.

Straneo, F. and Cenedese, C.: The dynamics of Greenland's glacial fjords and their role in climate. Annual review of marine science, 7(1), pp.89-112, https://doi.org/10.1146/annurev-marine-010213-135133, 2015.

https://doi.org/10.5194/egusphere-2026-5131
Preprint. Discussion started: 3 September 2026

Straneo, F. and Heimbach, P.: North Atlantic warming and the retreat of Greenland's outlet glaciers. Nature, 504(7478), pp.36-43, 2013.

Straneo, F., Sutherland, D.A., Holland, D., Gladish, C., Hamilton, G.S., Johnson, H.L., Rignot, E., Xu, Y. and Koppes, M.: Characteristics of ocean waters reaching Greenland's glaciers. Annals of Glaciology, 53(60), pp.202-210, doi:10.3189/2012AoG60A059, 2012.

Tremblay, J.É., Anderson, L.G., Matrai, P., Coupel, P., Bélanger, S., Michel, C. and Reigstad, M.: Global and regional drivers of nutrient supply, primary production and CO_2 drawdown in the changing Arctic Ocean. Progress in Oceanography, 139, pp.171-196, https://doi.org/10.1016/j.pocean.2015.08.009, 2015a.

Wassmann, P., Duarte, C.M., Agusti, S. and Sejr, M.K.: Footprints of climate change in the Arctic marine ecosystem. Global change biology, 17(2), pp.1235-1249, https://doi.org/10.1111/j.1365-2486.2010.02311.x, 2011.

Wassmann, P.: Overarching perspectives of contemporary and future ecosystems in the Arctic Ocean. Progress in Oceanography, 139, pp.1-12, doi:10.1016/j.pocean.2015.08.004, 2015.

Willis, J.K., Carroll, D., Fenty, I., Kohli, G., Khazendar, A., Rutherford, M., Trenholm, N. and Morlighem, M.: Ocean-ice interactions in Inglefield Gulf: Early results from NASA's Oceans Melting Greenland mission. Oceanography, 31(2), pp.100-108, 2018.

Zhu, Y., Suggett, D.J., Liu, C., He, J., Lin, L., Le, F., Ishizaka, J., Goes, J. and Hao, Q.: Primary productivity dynamics in the summer Arctic Ocean confirms broad regulation of the electron requirement for carbon fixation by light-phytoplankton community interaction. Frontiers in Marine Science, 6, p.275, https://doi.org/10.3389/fmars.2019.00275, 2019.